PyRe: A Cyclus Pyroprocessing Facility Archetype

Gregory T. Westphal and Kathryn D. Huff

Dept. of Nuclear, Plasma and Radiological Engineering, University of Illinois at Urbana-Champaign
gtw2@illinois.edu

ABSTRACT

Quantifying potential signatures and observables of material diverted from a pyroprocessing facility presents a modeling challenge. This work assesses system parameters that influence separation efficiency and throughput. We leverage these parameters to implement a customizable pyroprocessing facility archetype for use with the Cyclus framework. This generic facility model will allow simulations to quantify signatures and observables associated with various operational modes and material throughputs for a variety of facility designs. Such quantification can timely detection of material diversion. This paper describes the Pyre facility archetype design, pyroprocessing flowsheets captured by the model, and simulation capabilities it enables. To analyze data retrieved from the model, we propose a class for tracking and observing signatures and observables which will be extensible for other facility archetypes in the future.

INTRODUCTION

The diversion of significant quantities of special nuclear material from the nuclear fuel cycle is major non-proliferation concern [1]. These diversions must be detected in a timely manner using signatures and observables in order to properly safeguard the fuel cycle. Pyroprocessing is a used nuclear fuel separations technology capable of both converting current generation waste into sodium fast reactor fuel, and reprocessing next generation molten salt fuel types. With a new reprocessing technology comes new signatures and observables which in turn necessitate new diversion detection methods. The goal of this research is to identify potential signs of material diversion in a pyroprocessing facility and implement models of these processes into a detailed pyroprocessing facility archetype to the modular, agent-based, fuel cycle simulator, Cyclus [2]. This facility archetype will equip users of the Cyclus fuel cycle simulator to investigate the detection timeliness enabled by novel signatures and observables in various fuel cycle scenarios.

BACKGROUND: CYCLUS

Cyclus models the flow of material through agent-based user-defined nuclear scenarios. Facilities in nuclear fuel cycles vary, requiring a diverse collection of pre-designed facility process models, known as *archetypes*. Cycamore, the CYClus Additional MOdules REpository, provides the common facilities seen in simulations (separations, enrichment, reactor, etc.) [3]. Archetypes provide a mold for users to input values specific to each facility with a known output Cyclus can interpret. Simulations run in discrete time steps that allow exact isotopes to be dynamically tracked between facilities [2]. Tracking requires a form of signature or observable to follow the material accurately throughout and between facilities. Current capabilities would be truck deliveries, power draw, and steam production that have been proven sufficient for maximum likelihood estimations of diversion [4, 5]. Cyclus' discrete time allows users to investigate diversion and flag the time and location diversion occurs.

BACKGROUND: PYROPROCESSING

Pyroprocessing is an eletrochemical separation process used to recycle spent fuel into . With the capability of processing various forms of waste, efficiencies will differ according to design. There are four major systems within pyroprocessing with observable waste: voloxidation, electroreduction, electrorefining, electrowinning [6]. These processes have been defined by KAERI through their development of Pyroprocessing Integrated Demonstration (PRIDE) facility.

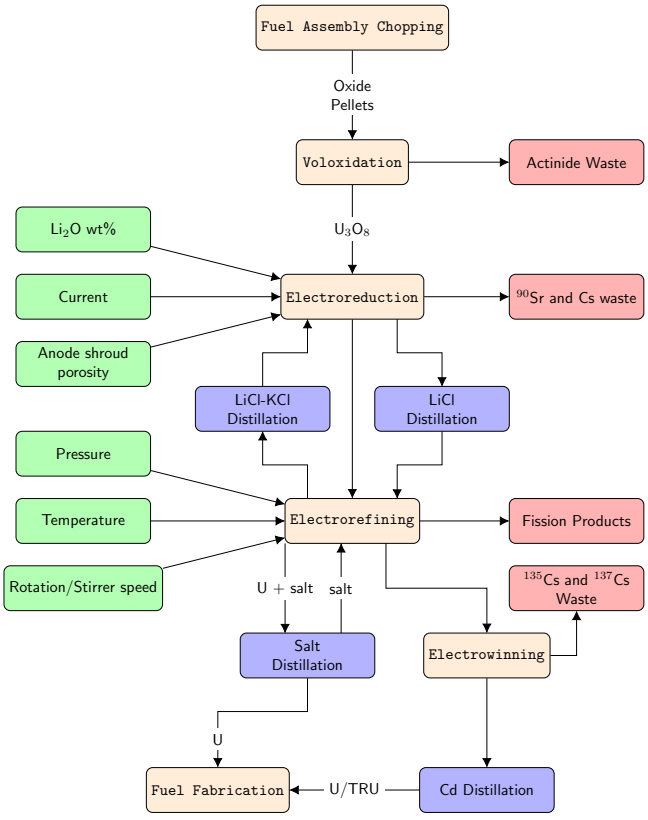

Fig. 1. An archetype design flowchart of pyroprocessing facilities including observable outputs and Cyclus variables.

Figure 1 demonstrates the primary separations steps in-

volved in a general pyroprocessing facility. Included are the process' main parameters along the left side of the flowsheet, each applied to processes most significantly impacted. The boxes on the right side of the processes contain the observable waste produced by each step that CYCLUS can track. Each of main processes are described below regarding information to be used by CYCLUS.

Voloxidation

Light Water Reactor (LWR) fuel must be initially treated and separated before proceeding with electrolytic processes. Heated under 500°C, noble gases and tritium are collected to decay in storage, and uranium dioxide is converted to U_3O_8. Actinides are also converted to their stable oxide forms and a majority are removed [7].

Electroreduction

Oxide pellets, created in voloxidation, enter the cathode metal basket. Voltage between 100 and 500 mA/cm^2 is applied to the anode in a molten LiCl salt. The electrolytic reduction process results in the diffusion of Cs, Ba and Sr primarily, along with the reduction and conversion of zirconium into metallic form [8, 7].

Electrorefining

Recoverable waste from reduction is fed into an anode basket suspended in a graphite cathode. LiCl-KCl eutectic is used as electrolyte above 500°C [7, 9]. The uranium dissolves at the anode to recombine at the cathode as metallic uranium. The lathanides and transuranic (TRU) waste are in a soluble chloride form while fission products and cladding remain in the anode basket. Finally, actinides and fission products are removed from the cladding electrochemically [9].

Electrowinning

The molten salt contains TRUs from electrorefining and are separated through electrowinning with trace uranium quantities. With a temperature of 500°C there is approximately 99 wt% reduction in actinides and lanthanides [7].

METHOD: CYCLUS SIMULATION

The separations facility provided by the CYCAMORE library expansion is used as an initial model of a simple PRIDE facility. The separations archetype allows for the declaration of a feed stream and requires the user-definition of facility efficiencies. Each waste stream requires a material balance over voloxidation, electroreduction, electrorefining and electrowinning. The main waste streams found are metallic waste, ceramic waste from electrowinning and electroreduction, and vitrified waste. Vitrified waste contains the majority of TRUs, Sr, and rare-earth elements. The efficiencies of each stream and their isotopes are determined through theoretical material balance determined by the NEA and Hermann et al [7, 10]. The simple simulation was run to verify the table of efficiencies input to CYCLUS.

A pyroprocessing facility can be adequately modeled through the separations archetype but does not have the detail afforded by a dedicated archetype. The goal for this archetype is to include the variations possible in facility configuration and their respective effects on the efficiency table. Efficiencies also vary according to the feed stream resulting in different waste streams for LWR and FR fuels, for example. Multiple material choices exist for anodes and cathodes as well as other design choices that require consideration.

Variations

It's important to consider variations in the construction of a pyroprocessing archetype since facility designs vary in multiple aspects which affect the throughput and efficiencies of different waste streams. Advanced methods for electrorefining developed by KAERI [11] further improve salt removal efficiencies and the effect of parameter variation. Temperature and pressure provide a significant improvement in removal efficiency, but can vary depending on facility specifications.

TABLE I: Under vacuum pressure, the evaporation coefficient and theoretical maximum removal efficiencies are calculated [11].

Vapor Pressure (mTorr)	Evaporation Coefficient	Salt Removal Efficiency
500	$3.04\text{x}10^{-5}$	97.3
300	$2.66\text{x}10^{-5}$	99.6
200	$1.25\text{x}10^{-4}$	99.4
100	$1.78\text{x}10^{-4}$	99.9

The data shown in Tables I and II are collected from KAERI's research into advanced electrochemical separation processes [11]. Salt removal efficiencies mentioned are concerned with the percentage of fission products and salt remaining in the uranium dendrites. The evaporation coefficient represents the amount of salt evaporated due to vacuum pressure. As shown by Table I, the addition of vacuum pressure to the system improves removal efficiency with a noticeable increase between 500 and 300 mTorr. Temperature, however, exhibits the opposite effect: as temperature decreases so does salt removal. This comes into effect particularly depending on material choice of instrumentation and containment. The most limiting material choice is iron because a eutectic forms between Fe and U at 725°C [12].

TABLE II: The evaporation coefficient and removal efficiencies are again calculated for varying temperature [11].

Temperature (C)	Evaporation Coefficient	Salt Removal Efficiency
1000	$1.25\text{x}10^{-4}$	99.4
900	$5.62\text{x}10^{-5}$	98.8
800	$4.63\text{x}10^{-5}$	94.9
700	$3.13\text{x}10^{-6}$	82.4

In facilities where iron equipment is present temperatures are limited to 700°C, and efficiency is significantly hindered. In these advanced processes, multiple cathodes surround an agitating central anode. Cathode arrangement and anode ro-

tation speed also affect the collection of uranium dendrites. Uneven, or sub-optimal, placement of cathodes result in an uneven electric field for electrolysis and lower efficiency while a high rotation speed causes remixing [11]. The addition of a central stirrer allows mixing of uranium dendrites stuck on the bottom of the vessel, improving separation efficiency and reducing the electroreduction time.

Throughput is also dependent on material choice for the inert electrodes whose operating voltages vary, impacting separation efficiency [13]. A shroud surrounds the anode to provide a path for O^{2-} ions to the anode and prevent Cl_2 from corroding the anode [14, 8]. Optimum operating current depends on the material choice for the anode shroud since a nonporous shroud limits ion pathways to the points of contact with the anode. Higher porosity corresponds to free ion paths and a higher current. With a higher current the separation time for reduction and winning are reduced [8].

Electroreduction can further improve its throughput by the addition of Li_2O as a catalyst and to prevent dissolution of the anode [8]. The catalyst often is used in concentration of 1 wt% with potential for up to 3 wt%. Since Li_2O is used to speed up the reaction, it is important to note that for signatures and observables the operators could add more oxide than reported to IAEA. More frequent shipments of lithium oxide can be tracked as an observable to match records.

METHOD: PROPOSED ALGORITHMS

Prior methodology explored by Hou et al. and Yilmaz et al. [4, 5] consists of minimum relative entropy based model and Poisson distribution respectively. Both methods are based on similar observables for the LWR fuel cycle. Enrichment facilities often have set production speeds for various enrichment levels and typical shipping options, expedited and standard. These production speeds can be monitored via IAEA inspection of waste activity or by monitoring facility power draw and smoke production. What becomes increasingly difficult is a minute increase in production that could be lost in the electrical noise of running a facility. For cases such as this where small diversions take place over an elongated period of time a fuel cycle simulation is beneficial. A nodal array of facilities and their known transport methods between each other is established [4]. Shipment times are combined with completion time for each enrichment level to develop a distribution of project completions. Hou et al. and Yilmaz et al. use these distributions to determine the likelihood of diversion through cumulative sum and maximum likelihood algorithms.

Scenarios without direct access to fuel orders require indirect observation by tracking the edges of a fuel cycle network. Increasing the number of known 'edges', or transportation routes, increases the algorithm speed with the only monitoring points as intake and output of facilities. Figure 2 demonstrates a partially observed network to which a hybrid minimum relative entropy model is applied. This technique results in a more lenient input compared to a maximum likelihood estimation that requires a majority of the network to be observed [4].

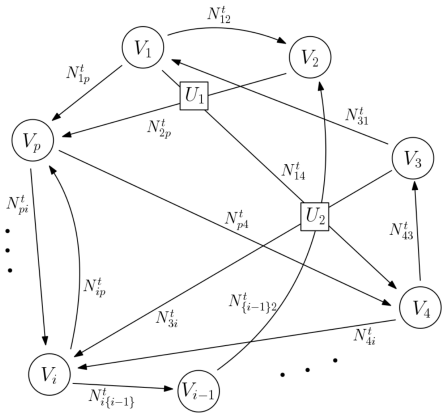

Fig. 2. Shadow transactions acting on a facility array by Hou et al[4].

DISCUSSION

Using a material balance area over electrorefining and electroreduction yields the majority of detectable waste from the electrochemical processes. Electroreduction produces the majority of Sr and Cs waste with a considerable decay signature proportional to the efficiency and size of the feed batch [6, 7]. The electrorefining process also produces the fission product waste stream which requires monitoring. The following products are produced and tracked in this step: Tc, Ag, Pd, Rh, Ru, Mo and Zr [7]. Material balances over the remaining processes are used to verify diversion did not occur. Electrowinning produces Cs waste similar to electroreduction except in reduced quantities. Fuel fabrication is of high risk since finished product can be diverted with no additional processing steps, therefore a material balance must also be taken here.

To determine the most significant places of diversion and where to observe them, multiple scenarios must be considered. Each facility parameter must be varied to observe their effects, as well as using a limited number of material balance areas. Scenarios will be run that include various monitoring points with the goal of determining if excess material was produced and what parameter was altered. For example, an increase in Cs production points to electroreduction and electrowinning. If both increase similarly then current is likely affected as these processes share an increase efficiency with increased current. Further in this scenario, if Cs production increases while Sr does not, electrowinning must be the point at which parameters are altered. A set of these scenarios will be used for sensitivity and importance analysis on the generic pyroprocessing facility.

CONCLUSIONS

This analysis demonstrates the variability in commercialized pyroprocessing facilities and their affects on potential signatures and observables that will be tracked through a detailed archetype. CYCLUS also is outlined as tool in detecting shadow fuel cycles through its agent-based simulation and modular facilities, allowing for variations in plant design. Modeling and data collection of shadow fuel cycles will be performed in the

CYCLUS environment after creation of a library specific to the unique needs of electrochemical refinement. Data from these simulations will be utilized in a minimum relative entropy model with additional signatures and observables to inform on detector placements and measurement points leading to more reliable diversion detection.

ACKNOWLEDGMENTS

This research was performed using funding received from the Consortium for Nonproliferation Enabling Capabilities under award number 1-483313-973000-191100.

REFERENCES

1. "IAEA Safeguards: Serving Nuclear Non-Proliferation," Tech. rep., IAEA (Dec. 2017).
2. K. D. HUFF, M. J. GIDDEN, R. W. CARLSEN, R. R. FLANAGAN, M. B. MCGARRY, A. C. OPOTOWSKY, E. A. SCHNEIDER, A. M. SCOPATZ, and P. P. H. WILSON, "Fundamental concepts in the Cyclus nuclear fuel cycle simulation framework," *Advances in Engineering Software*, **94**, 46–59 (Apr. 2016).
3. K. D. HUFF, M. FRATONI, and H. R. GREENBERG, "Extensions to the cyclus ecosystem in support of market-driven transition capability," Tech. rep., Lawrence Livermore National Laboratory (LLNL), Livermore, CA (2014).
4. E. HOU, Y. YILMAZ, and A. O. HERO, "Diversion Detection in Partially Observed Nuclear Fuel Cycle Networks," (2016).
5. Y. YILMAZ, E. HOU, and A. O. HERO, "Online Diversion Detection in Nuclear Fuel Cycles via Multimodal Observations," (2016).
6. R. A. BORRELLI, J. AHN, and Y. HWANG, "Approaches to a Practical Systems Assessment for Safeguardability of Advanced Nuclear Fuel Cycles," *Nuclear Technology*, **197**, 248–264 (Mar. 2017).
7. ORGANISATION FOR ECONOMIC CO-OPERATION AND DEVELOPMENT, "Spent Nuclear Fuel Reprocessing Flowsheet," *Nuclear Energy Agency* (Jun. 2012).
8. E.-Y. CHOI and S. M. JEONG, "Electrochemical processing of spent nuclear fuels: An overview of oxide reduction in pyroprocessing technology," *Progress in Natural Science: Materials International*, **25**, *6*, 572–582 (Dec. 2015).
9. H. LEE, J.-M. HUR, J.-G. KIM, D.-H. AHN, Y.-Z. CHO, and S.-W. PAEK, "Korean Pyrochemical Process R&D activities," *Energy Procedia*, **7**, 391–395 (2011).
10. S. D. HERRMANN and S. X. LI, "Separation and Recovery of Uranium Metal from Spent Light Water Reactor Fuel Via Electrolytic Reduction and Electrorefining," *Nuclear Technology*, **171**, *3*, 247–265 (Sep. 2010).
11. H. LEE, J. H. LEE, S. B. PARK, Y. S. LEE, E. H. KIM, and S. W. PARK, "Advanced Electrorefining Process at KAERI," .
12. L. CHAPMAN and C. HOLCOMBE, "Revision of the uranium-iron phase diagram," *Journal of Nuclear Materials*, **126**, *3*, 323–326 (Nov. 1984).
13. T. KOYAMA, Y. SAKAMURA, M. IIZUKA, T. KATO, T. MURAKAMI, and J.-P. GLATZ, "Development of Pyro-processing Fuel Cycle Technology for Closing Actinide Cycle," *Procedia Chemistry*, **7**, 772–778 (2012).
14. T.-J. KIM, G.-Y. KIM, D. YOON, D.-H. AHN, and S. PAEK, "Development of an anode structure consisting of graphite tubes and a SiC shroud for the electrowinning process in molten salt," *Journal of Radioanalytical and Nuclear Chemistry*, **295**, *3*, 1855–1859 (Mar. 2013).